Polymerization of Propylene by a New Generation of Iron Catalysts: Mechanisms of Chain Initiation, Propagation, and Termination

Brooke L. Small and Maurice Brookhart*

Department of Chemistry, University of North Carolina at Chapel Hill, Chapel Hill, North Carolina 27599-3290

Received October 29, 1998; Revised Manuscript Received January 13, 1999

ABSTRACT: A new series of iron catalysts bearing tridentate pyridine−bis(imine) ligands are reported for the isospecific polymerization of propylene (PP). The catalytic activities are moderate, with maximum activities exceeding 1600 kg PP/mol Fe h under 1 atm of propylene pressure at −20 °C . End-group analyses of the resultant materials are performed and indicate that the polymerization proceeds via a 2,1 mechanism of propagation leading to the exclusive formation of 1-propenyl end groups following β-H elimination/ abstraction and chain transfer. The polymers are highly regioregular, but the regioregularity decreases with decreasing steric bulk of the tridentate ligands. Isotacticities are determined for a number of catalysts bearing ligands with variable ortho substituent patterns and symmetries. In all cases, isotactic material is obtained; the $[m]^4$ methyl pentad content is always in the range of 55−67%. ^{13}C NMR spectroscopy is used to demonstrate that the isotacticity arises from a chain-end control mechanism. These catalysts represent the first isospecific systems known to operate by a 2,1 mechanism of propagation.

Introduction

The polymerization of propylene by soluble transition-metal complexes is an area of intense interest.[1] The various properties of polypropylenes produced by modifications in catalyst structure or reaction conditions are a result of changes in tacticity,[1] regioregularity,[2] molecular weight,[3] stereoblock length and distribution,[4] and type and degree of branching.[5] Thus, many studies have been undertaken to understand the mechanisms that regulate the formation of polymer.

A new series of iron and cobalt catalysts that are highly active for the polymerization of ethylene was recently reported by Gibson,[6] DuPont,[7a] and this group.[7b] We have also reported that less sterically bulky variations of the iron catalysts are extremely active and selective for the oligomerization of ethylene to linear α-olefins[8] and that the iron-based polymerization systems are moderately active for the production of polypropylene.[9] The polypropylenes previously reported possess reasonable degrees of isotacticity (% $[m]^4$ > 50%) and exhibit ^{13}C NMR resonances in the methyl pentad region consistent with a mechanism of propagation governed by chain-end control.[9] Herein, we report the effects that changes in catalyst structure and reaction conditions have on the stereochemistry, regiochemistry, and molecular weight of the polymers and the activities of the catalysts. Additionally, end-group analyses are performed on the polymers to gain a better understanding of the mechanisms that govern intitiation, propagation, and chain transfer.

Results and Discussion

Synthesis of Complexes 1−9. The precatalyst complexes are pentacoordinate species of the general formula {[(ArN=C(Me))$_2$C$_5$H$_3$N]FeCl$_2$} (Ar = alkyl-substituted aryl ring), consisting of a pyridine−bis(imine) ligand coordinated to iron (II) chloride (Figure 1). The syntheses of complexes 1−3 were reported previously,[7b] and complexes 4−9 are made by the same method; namely, the addition of a slight excess of the
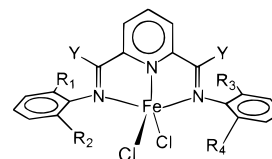
1 R$_1$ = R$_2$ = R$_3$ = R$_4$ = *i*Pr, Y = CH$_3$
2 R$_1$ = R$_2$ = R$_3$ = R$_4$ = CH$_3$, Y = CH$_3$
3 R$_1$ = R$_3$ = *t*Bu, R$_2$ = R$_4$ = H, Y = CH$_3$
4 R$_1$ = *t*Bu, R$_2$ = H, R$_3$ = R$_4$ = CH$_3$, Y = CH$_3$
5 R$_1$ = *t*Bu, R$_2$ = H, R$_3$ = R$_4$ = *i*Pr, Y = CH$_3$
6 R$_1$ = R$_3$ = *i*Pr, R$_2$ = R$_4$ = CH$_3$, Y = CH$_3$
7 R$_1$ = R$_2$ = *i*Pr, R$_3$ = R$_4$ = CH$_3$, Y = CH$_3$
8 R$_1$ = R$_3$ = *i*Pr, R$_2$ = R$_4$ = CH$_3$, Y = H
9 R$_1$ = R$_2$ = R$_3$ = *i*Pr, R$_4$ = CH$_3$, Y = CH$_3$

Figure 1. Iron complexes used for the polymerization of propylene. See Table 2 for pictorial representations of these complexes.

ligand to the hydrated or anhydrous form of the iron salt in THF. The reactions are complete in all cases in less than 2 h, and the products are isolated by filtration or evaporation and washed with ether and pentane to generate the precatalysts in near quantitative yields. The syntheses for ligands 4′−9′ used to make complexes 4−9 are reported in the Experimental Section.

Polymerization Studies: Relationship of Catalyst Structure to Activities and Polymer Molecular Weights. Data for the polymerization of propylene using precatalysts 1−9 are presented in Table 1. The polymerizations were carried out in toluene using modified methylalumoxane (MMAO)[10] as the cocatalyst under 1 atm of propylene (Scheme 1). As in the case of *ethylene* polymerization by iron-,[6,7] cobalt-,[6,7] nickel-,[5d,11] and palladium-based[5d,11] diimine catalysts, the main factor governing the molecular weight of the polypropylenes is the steric bulk of the ligands. Complex **1**, which contains four *o*-isopropyl substituents on the aryl rings, produces polypropylene at −20 °C with an M_n of 6500 (Table 1, entry 2). Complex 9, with slightly reduced steric congestion, results in polymer with an M_n of 5700 (entry 18). Further reductions in the size of the ortho substituents yield lower molecular weight polymers, as

Table 1. Data for the Polymerization of Propylene[a]

entry	pre-catalyst	loading (μmol)	T (°C)	M_n ($\times 10^{-3}$)	M_w/M_n	TOF ($\times 10^{-3}$/h)	yield (g)
1	**1**	3.5	0	3.7	2.3	4.1	1.18
2		3.8	−20	6.5	2.1	12.9	4.10
3	**2**	4.2	0	1.7	2.1	6.9	2.45
4		4.6	−20	1.8	2.3	3.0	1.16
5	**3**	3.8	0	1.2	2.2	1.6	0.50
6		4.2	−20	1.7	2.1	6.5	2.28
7	**4**	4.0	0	2.0	2.4	6.9	2.31
8		4.0	−20	2.7	1.8	7.3	2.46
9	**5**	3.6	0	1.1	2.2	1.1	0.33
10		4.1	−20	2.0	2.2	3.1	1.09
11	**6**	3.8	0	2.9	2.0	10.4	3.33
12		4.0	−20	4.1	2.2	17.3	5.78
13	**7**	3.8	0	3.5	2.5	7.0	2.25
14		3.8	−20	5.6	2.2	38.8	7.24
15	**8**	4.2	0	0.6	2.1	0.5	0.19
16		4.2	−20	1.2	1.9	0.7	0.25
17	**9**	3.4	0	2.8	2.1	4.7	1.36
18		3.4	−20	5.7	1.8	11.8	3.42

[a] All runs were done using 1 atm propylene and 50 mL of toluene with MMAO as cocatalyst. Each polymerization was run for 120 min, with the exception of entry 14 which was run for 70 min because of stirring difficulties.

Scheme 1
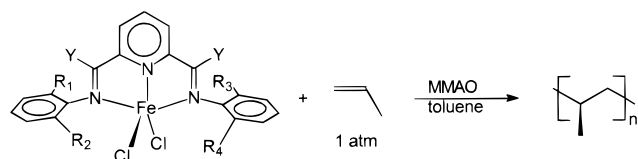
evidenced by the results from activated catalysts **6** and **7**. Each system contains two *o*-methyl groups and two *o*-isopropyl groups, and polymers with M_n's of 4100 and 5600, respectively, are obtained (entries 12 and 14). Complex **2**, with four *o*-methyl substituents, demonstrates this trend conclusively by yielding polypropylene with an M_n of 1800 (entry 4) under the same conditions as the other catalysts.

Raising the temperature of the polymerization results in decreased molecular weights, a trend exhibited by all catalysts **1**−**9**. As has been reported for ethylene polymerization,[7b,8] it is likely that the rates of chain growth and chain transfer are both first-order in the monomer, so that, assuming similar entropies of activation, an increase in the reaction temperature will result in a decrease in the k_p/k_t ratio (propagation rate/chain transfer rate) and a decrease in M_n.

On the basis of the GPC data, all of the polymers reported have relatively low molecular weights, with M_n's ranging from ∼600−7000. All of the polydispersities reported in Table 1 are monomodal and near 2.0, the expected value for polyolefins made via single-site catalysts when the M_n value is limited by the rate of chain transfer.[12] In the case of ethylene polymerization,[7b] low molecular weights were explained by a mechanism in which propagating chains could transfer to the aluminum activator,[13] resulting in very broad or even bimodal polydispersities. Chain transfer to aluminum, therefore, does not appear to play a dominant role in these chain terminations. The implications of these observations will be discussed later.

In most cases the total turnovers (TOs) after 120 min reaction time are higher at −20 °C than at 0 °C. This fact is probably largely due to the much higher solubility of propylene in toluene at the lower temperature (resulting in higher turn-over *frequencies*, TOFs), but

catalyst lifetime undoubtedly plays an important role. Both the reaction temperature and the steric bulk of the *o*-substituents seem to play a role in determining catalyst lifetimes. Upon activation with MMAO, complex **2** polymerizes propylene with little loss in activity over 24 h at 0 °C, but the bulkier **1** (Table 1, entry 1) is almost completely deactivated after 2 h. at the same temperature. However, performing the polymerization at −20 °C with **1**/MMAO results in a system that is still quite active after 2 h (entry 2). Entries 1 and 2 (catalyst **1**) in Table 1 show a 3-fold increase in the total turnovers 2 h after the temperature is lowered (8200 at 0 °C vs 25 800 at −20 °C), whereas entries 3 and 4 (catalyst **2**) actually exhibit the opposite trend, showing over a 50% decrease in the turnover number after the temperature is lowered (13 800 at 0 °C vs 6000 at −20 °C). Apparently, the lifetimes of the sterically bulkier systems are substantially reduced by raising the reaction temperature. Thus, the initial *activities* (TOFs) of the bulky **1** and the less bulky **2** are quite similar at 0 °C, but catalyst **2** has a longer *sustained* activity (more total TOs) under these conditions. The lower activity of catalyst **2** at −20 °C may be due to poor solubility of this less congested complex at low temperatures. The most active catalyst was **7**, which had a turnover frequency of 39 000/h at −20 °C (Table 1, entry 14), corresponding to an activity of 1640 kg polypropylene/mol catalyst h.

The Effect of Catalyst Structure on Polymer Microstructure. In early metal-catalyzed polymerizations of α-olefins, symmetry modifications and other structural variations of the catalysts have been shown to have a dramatic and often predictable effect on the polymer microstructure.[1] In general, achiral complexes such as Cp$_2$TiPh$_2$ will polymerize propylene in an atactic fashion; however, Ewen's classic paper[14] demonstrated that at low temperatures this system, upon activation, produces moderately isotactic polymers (52% [m][4] at −45 °C). Examination of the ^{13}C NMR methyl pentad region showed clearly that the tacticity arose from a chain-end control mechanism,[15] in which the last inserted monomer unit controlled the stereochemistry of propagation.

Additionally, prochiral monomers such as propylene may be enchained via an enantiomorphic site-control mechanism,[16] in which the ancillary ligands dictate the stereochemistry of successive insertions. In the case of site control, metallocene complexes possessing C_2 symmetry can be highly effective in producing isotactic polymers, whereas some complexes having C_s symmetry are able to make syndiotactic polymers. Certain catalysts possessing C_1 symmetry are also known to exhibit isospecificity via a site-control mechanism.[1] It has been demonstrated that these trends relating to catalyst symmetry are not rigid requirements,[17] but clearly, the work of Brintzinger,[18] Ewen,[19] Kaminsky,[20] Waymouth,[4] Bercaw,[21] and others[1,22] has shown how closely related the concept of catalyst symmetry is to the resultant polymer microstructure.

Keeping this pioneering work with metallocenes in mind, we have investigated the effects of varying ligand structures and symmetries on the microstructures of the polypropylenes produced. The series of asymmetric alkyl substituted ligands **4′**−**9′** was synthesized. ^{13}C NMR spectra of these ligands are quite diagnostic, revealing that rotations of the ortho-disubstituted aryl rings do not occur on the NMR time scale at room temperature (rates less than ca. 10 s^{-1}). For example, ligand **7′**
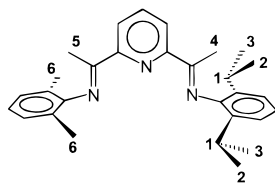
Figure 2. Labeling of chemically nonequivalent carbons of **7′**.
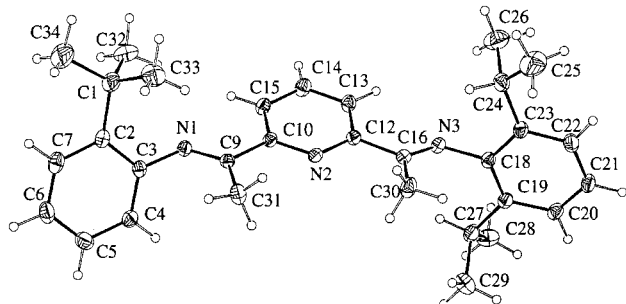
Figure 3. X-ray crystal structure of **5′**. Selected bond distances (Å) and torsion angles (deg): C(12)−C(16), 1.495(3); C(10)−C(9), 1.491(3); C(16)−N(3), 1.273(3); C(9)−N(1), 1.284(3); N(3)−C(18), 1.429(3); N(1)−C(3), 1.416(3); C(31)−C(9)−C(10)−C(15), 174.0(5); C(30)−C(16)−C(12)−C(13), 169.3(5); C(16)−N(3)−C(18)−C(23), 87.1(4); C(16)−N(3)−C(18)−C(19), 99.7(4); C(9)−N(1)−C(3)−C(2), 118.4(5); C(9)−N(1)−C(3)−C(4), 69.5-(4).

exhibits six resonances in the upfield region of the ^{13}C NMR spectrum, and ligand **6′** has five signals in the same range with only one observable isomer. If rotation were rapid, equilibration of the isopropyl methyl groups would be observed, resulting in the appearance of five and four signals in the ^{13}C NMR alkyl region for **7′** and **6′**, respectively. Figure 2, in which the alkyl carbons are labeled for **7′** with "locked" aryl rings, is provided to further clarify this discussion.

Apparently, removal of the steric bulk afforded by the imine methyl groups results in much lower rotational barriers of the aryl rings. Ligand **8′**, made from 2,6-pyridinedicarboxaldehyde and 2-isopropyl-6-methyl-aniline, shows three resonances in the ^{13}C NMR alkyl region, a result consistent with rapid aryl ring rotation. Additionally, ^{13}C NMR spectroscopy has been used to demonstrate that aryl rings containing only one ortho substituent, such as **3′−5′**, will rapidly rotate on the NMR time scale, which results in site exchange of the substituents on the other ring. Ligand **5′**, having one *o-tert*-butyl group on one ring and two isopropyl groups on the other ring, exhibits six signals in the upfield ^{13}C NMR region (25 °C), suggestive of rapid rotation of the *tert*-butyl-substituted ring. Crystals of **5′** suitable for X-ray analysis were obtained by slowly cooling a solution of the ligand in hot isopropyl alcohol. Figure 3 shows the ORTEP structure for this compound.[23] In the solid state, the most interesting feature of this asymmetric ligand is the conformation of the substituents attached to the 2 and 6 (C10 and C12 on ORTEP) positions of the pyridine ring. These groups are rotated about 180°from the position they must occupy to chelate the metal.

The ligands **1′−9′**, by means of variable substitution patterns, possess different symmetries that are assigned based on the U-shaped ligand configurations seen in the complexes (see Figure 2), with the aryl groups orthogonal to the N−N−N plane. Table 2 lists ligand symmetries in complexes **1−9**. The NMR analyses of the

Table 2. Ligand Symmetries in Complexes 1−9

complex	structure	ligand symmetry
1		C_{2v}
2		C_{2v}
3		C_s/C_2
4		C_1
5		C_1
6		C_s[a]
7		C_s
8[b]		C_s/C_2[c]
9		C_1

[a] The symmetry of the ligand coordinated to **6** was established by X-ray crystallography (Figure 4). [b] Note that **8** possesses H rather than CH$_3$ substituents on the imine carbons. [c] Rapid rotation of the aryl rings in the free ligand is observed by ^{13}C NMR spectroscopy due to the less bulky H's on the imine carbons.

free ligands and results obtained for similar Ni and Pd α-diimine complexes[24] indicate that when an aryl group is substituted at *both o*-positions and the imine carbons bear a methyl group, the barrier to aryl ring rotation will be high and the ring will be effectively locked on the time scale of polymerization. Two isomeric complexes thus may be formed from ligand **6′**, although only a single isomer is observed by NMR spectroscopy (see above) for the isolated free ligand. X-ray analysis of complex **6a**, isolated during the synthesis of **6**, suggests that the ligand binds to iron in the C_s configuration. The ORTEP structure of **6a** is shown in Figure 4.[25] Because of a reaction with solvent and/or moisture during crystallization,[26] a second iron center is seen in which an FeCl$_3$ unit is bridged to the imine-ligated iron atom via an oxygen atom. On the basis of our prior work, the bridging group is likely an OH.[27] These results suggest that complex **6** used in polymerization possesses a ligand with C_s symmetry, but we cannot rule out the possibility that both complexes (C_s and C_2) are present in the crude product and that only one readily crystallizes.

In complex **3**, which possesses a single *o*-substituent, as well as in complex **8**, prepared from the pyridine dialdehyde with Y = H (see Figure 1), the barrier to aryl rotation is expected to be lower (see above) and two rapidly equilibrating, interconverting isomers may be present in solution during polymerization (Table 2). For complex **1**,[7] the X-ray structure showed it possessed formal C_s symmetry because of the pseudosquare pyramidal arrangement of the ligands around the central atom. However, the free ligand **1′** possesses formal C_{2v} symmetry. As a final point regarding the ligand symmetries in complexes **1−9**, note that ligands **6′** and **7′**,
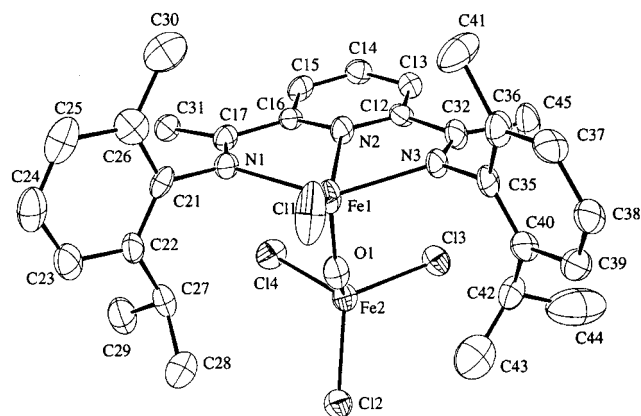
Figure 4. X-ray crystal structure of **6**. Selected bond distances (Å) and angles (deg): Fe(1)−N(1), 2.197(7); Fe(1)−N(2), 2.076-(7); Fe(1)−N(3), 2.163(7); Fe(1)−Cl(1), 1.179(3); Fe(1)−O(1), 1.769(8); Fe(2)−O(1), 1.765(7); Cl(1)−Fe(1)−O(1), 113.58(24); N(1)−Fe(1)−Cl(1), 98.89(23); N(3)−Fe(1)−Cl(1), 98.74(23); N(2)−Fe(1)−O(1), 99.0(3); N(1)−Fe(1)−N(3), 144.0(3); N(1)−Fe(1)−N(2), 74.4(3).

although having the same C_s symmetry, possess mirror planes that are orthogonal to each other.

Polymerization of propylene was carried out with complexes **1**−**9**, and the resultant polymers were analyzed by ^{13}C NMR spectroscopy to determine the effects of catalyst structure on polymer stereochemistry. Figure 5a−e shows the ^{13}C NMR methyl pentad region for a series of polypropylenes made at −20 °C . Although all of the polymers made by catalysts **1**−**9** are isotactic, the spectra shown in Figure 5 represent the higher molecular weight samples made by the more bulky systems. These higher molecular weights, combined with the high regioregularity of the polypropylenes, allowed for straightforward comparative analysis of the methyl pentad spectra. Figure 5a indicates that the polypropylene made by complex 1/MMAO has about 55% $[m]^4$ content, corresponding to a probability of successive stereoregular insertions of 0.86 (P[m] = $^4\sqrt{[m]^4}$). The labeled small pentads representing mistakes in the isotactic sequences are entirely consistent with a chain-end control mechanism.[14,15] These mistakes arise when the monomer inserts into the polymer chain to form an *r* dyad instead of the usual *m* dyad. In a site-control mechanism, this inversion of stereochemistry would be rectified by the catalyst center, resulting in a retention of the absolute stereochemistry of the chain and the overall generation of an *rr* triad. In a chain-end control mechanism, propagation is governed by the monomer unit inserted last, so the stereoerror would continue to be propagated in the ensuing insertion, resulting in the generation of an *rm* triad. The identification of these errors, shown using modified Fischer projections in Figure 6, allows for the classification of the mechanism. At the pentad level, site-control systems will exhibit *mmmr*, *mmrr*, and *mrrm* errors in a 2:2:1 ratio, and catalysts that operate by a chain-end control mechanism will contain *mmmr* and *mmrm* pentads as the major errors in a 1:1 ratio. Figure 5a clearly indicates that the stereoerrors generated by catalyst **1** are a result of chain-end control. The degree of isotacticity is very similar to that seen by Ewen[14] using Cp₂TiPh₂/MAO at −45 °C. However, the isospecificity of Ewen's system decreased substantially at elevated temperatures (52% $[m]^4$ at −45 °C and 34% $[m]^4$ at −15 °C), with nearly atactic polymers forming at 0 °C.
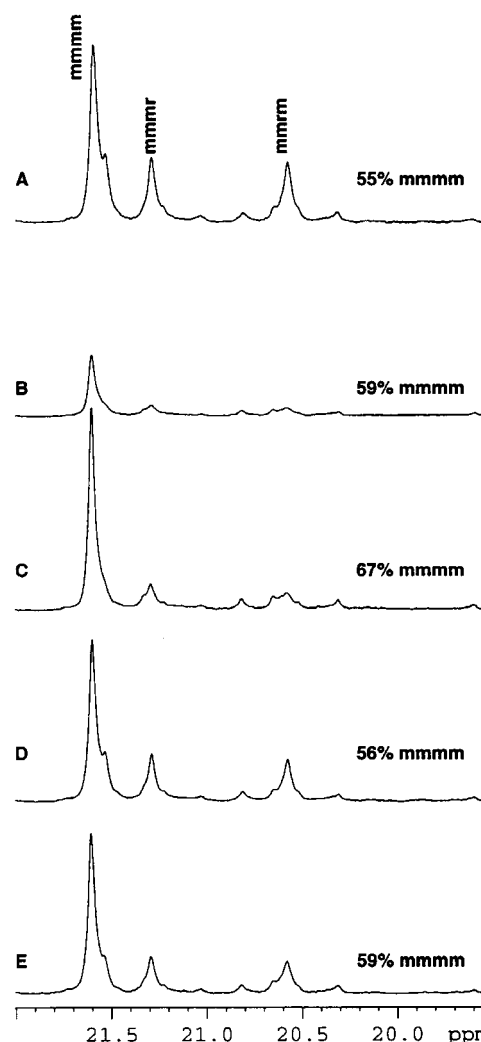
Figure 5. ^{13}C NMR spectra of methyl pentad regions for polypropylenes made at −20 °C. All complexes were activated with MMAO. (a) Catalyst **1**, (b) catalyst **5**, (c) catalyst **6**, (d) catalyst **7**, and (e) catalyst **9**.
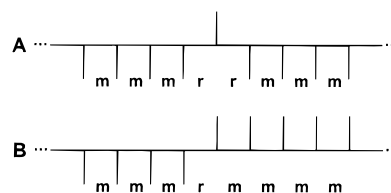
Figure 6. Modified Fischer projection showing major errors in (a) site-controlled and (b) chain-end controlled polymerization processes.

Figure 5b shows the ^{13}C NMR methyl pentad region of polypropylene made by C_1-symmetric **5** under the same conditions (−20 °C, 1 atm propylene). The spectrum looks remarkably similar to the spectrum in Figure 5a, but indicates a slightly higher $[m]^4$ content of 59%, corresponding to a meso dyad probability of 0.88. In fact, Table 3 shows that none of the catalysts investigated was able to significantly influence enchainment in a predictable manner toward higher isotactic (or even syndiotactic) content. Catalysts **5** (Figure 5b) and **9** (Figure 5e), both having C_1 symmetry, yielded polypropylene with 59% $[m]^4$ content, and catalysts **6** (Figure 5c) and **7** (Figure 5d), with C_s symmetry, produced polymers with 67 and 56% $[m]^4$ compositions, respectively. Column 2 of Table 3 indicates that these

Table 3. Stereoregularity of Propylene Polymerization at −20 °C

| catalyst	$P_m{}^a$	% [m][4]
1	86	55
5	88	59
6	91	67
7	87	56
9	88	59

[a] Probability of a meso dyad.

small disparities in isotacticity become even smaller when the dyad contents are considered, with the P_m values ranging from 0.86 for catalyst **1** to 0.91 for catalyst **6**. It is now clear, as the overlaid spectra in Figure 5 indicate, that the chain-end control mechanism operates preferentially regardless of the steric and symmetry modifications introduced into complexes **1**−**9**. These observations are in marked contrast to the results obtained with metallocene catalysts, in which the catalyst structure is known to greatly influence the polymer microstructure.

^{13}C and ^{1}H NMR Analysis of End Groups: Modes of Initiation, Propagation, and Chain Termination. Although direct observation of migratory insertion reactions and catalytic intermediates can provide critical mechanistic details[28] relating to a particular polymerization system, spectroscopic analysis of the polymers formed is also a powerful tool for understanding how catalysts work. The polypropylenes reported herein were subjected to detailed ^{13}C and ^{1}H NMR studies to gain insights into the initiation, propagation, and termination steps.

Figure 7a is the ^{13}C NMR spectrum of polymer made by **1** at −20 °C (Table 1, entry 2). The polymer is highly regioregular, with no resonances indicative of tail-to-tail,[2d] head-to-head,[2d] or 1,3-enchainment.[2d,e] No relaxation delay was used for this sample in order to minimize observation of the end groups, which can have T_1's up to 5 s.[29a] Figure 7b is the spectrum of polypropylene made by **2** at −20 °C (Table 1, entry 4). Unlike

the polymers made using the more sterically hindered catalysts, this sample contains a small amount of regioerrors, denoted by the signals with asterisks near 15.5−17.5, 34.0−36.5, and 40.0−41.7 ppm.[2d] These regiomistakes, however, are the exception rather than the rule in these systems, because they only occur in systems with sterically small *o*-substituents (complexes **2**−**4** and **8**).

Signals attributable to the polymer end groups can also be observed in these polypropylenes as a result of the low molecular weight of the samples. Figure 8 is the ^{1}H NMR spectrum in the olefinic region of polypropylene made by **3** at −20 °C. This spectrum is representative of all of the proton spectra and shows that catalysts **1**−**9** produce polymers with exclusively α-olefin end groups (i.e., no internal olefin or vinylidene end groups). Scheme 2 indicates the various processes that can lead to α-olefin end groups. A β-H elimination followed by chain displacement after successive 1,2 and 2,1 insertions will lead to a 1-butenyl end group (Scheme 2, process 1); and β-CH$_3$ elimination and chain transfer following successive 1,2 insertions will produce a 1-propenyl (allyl) end group (Scheme 2, process 2). Alternatively, an allyl end group may also form via β-H elimination[3c,30] after successive 2,1 insertions (Scheme 2, process 3). Therefore, the first goal was to determine the nature of the unsaturated chain end. Figure 9a is the ^{13}C DEPT 135 spectrum of polypropylene made by 1 at 0 °C. The polymer retains its stereo- and regioregularity at this temperature; however, polymerization at 0 °C leads to lower molecular weight and more soluble polymers that facilitate end group analysis. A single methine resonance at 137.6 ppm and a single methylene signal at 115.8 ppm (Figure 9a inset) indicate that only one type of olefinic end group is present. These resonances coincide more closely with the olefinic resonances of 4-methylpentene (137.4 and 115.3 ppm) than with the corresponding peaks of 1-hexene (138.7 and 114.1 ppm), thus suggesting the presence of an allyl end group. In
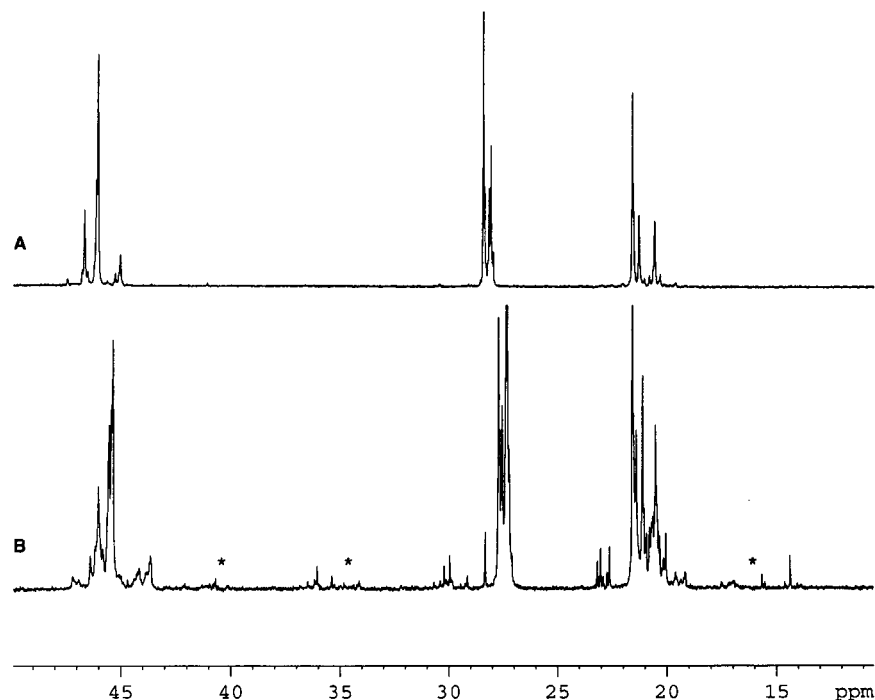
Figure 7. ^{13}C NMR spectrum of polypropylenes made by (a) **1**/MMAO at −20 °C (C$_6$D$_5$Br NMR solvent) and (b) **2**/MMAO at −20 °C (1,1,2,2-dideuteriotetrachloroethane NMR solvent). Regioerrors are observed in the lower molecular weight material.
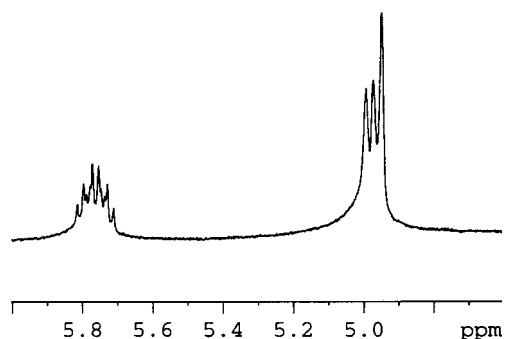
Figure 8. ^{1}H NMR of olefinic region of polypropylene made by **3**/MMAO at −20 °C .

the aliphatic region of the spectrum, C3 of the allyl end group is assigned at 40.8 ppm, on the basis of the DEPT spectrum, comparison to literature values,[29] favorable comparison to C3 of 4-methylpentene (43.3 ppm),[31] and the generation of an *n*-propyl saturated end group upon hydrogenation (described later). C4 of the allyl end group is assigned at 30.0 ppm, where it is nearly coincidental with another resonance.

^{1}H NMR spectroscopy was also used to verify the nature of the olefinic end group. Figure 10 shows a labeling scheme for the two possible types of end groups. In either case, H_d and H_e are diastereotopic, and identification of their respective resonances in combination with decoupling experiments was used to prove that this C3 methylene group is adjacent to a *methine* group at C4. To perform this experiment, a polymer with sufficiently low molecular weight was selected (Table 1, entry 6), and H_d and H_e were identified as multiplets centered at 1.83 and 2.08 ppm. Decoupling of H_c reduced these signals to doublets of doublets, with a geminal $J(H_d−H_e)$ coupling constant of 13.0 Hz and $J(H_d−H_f)$ and $J(H_e−H_f)$ coupling constants of 8.4 and 4.5 Hz, respectively. The multiplicities of these peaks as well as the observed coupling constants are consistent with a diastereotopic methylene group being next to a methine group and provide further evidence for allyl end groups. At this point, it was possible to rule out process 1 of Scheme 2 as the chain-transfer step.

With good evidence supporting the exclusive existence of 1-propenyl end groups, it was necessary to examine the saturated chain ends to gain information about initiation. The ^{13}C DEPT spectrum in Figure 9a combined with comparison to literature data was helpful in this regard. The observed resonances at 14.4, 23.2, 29.2, 36.1, and 30.0 ppm were not consistent with isobutyl[32] or *n*-propyl[33] end groups. The work of

Hayashi,[34] Cheng and Smith,[29a] and Sacchi[29b] clearly indicate these resonances are due to *n*-butyl end groups, thereby eliminating process 2 of Scheme 2 as the chain transfer process. $β$-CH₃ elimination could not lead to *n*-butyl end groups without 1,3-enchainment, but we see no evidence of chain straightening. Figure 9a illustrates the proposed assignments for these *n*-butyl resonances, and Table 4 is provided to indicate the numbering scheme used and to tabulate the data from Figure 9a−d. In addition to these lines, three other resonances at 22.7, 23.1, and 28.4 ppm are observed. These resonances agree closely with what would be expected for an isopentyl (3-methylbutyl) end group,[29] which could be formed by transfer of an isobutyl group from the MMAO activator to the metal center, followed by initiation via 2,1 insertion. To test this hypothesis, the polymerization was run using triethylaluminum and tris(perfluorophenyl)borane as the cocatalyst. This modified activator system led to the disappearance of the 3-methylbutyl resonances and to the appearance of new signals consistent with the *exclusive* formation of *n*-propyl groups at the saturated chain ends with an equal number of unsaturated allyl end groups. The ^{13}C DEPT spectrum for this experiment is shown in Figure 9b, with the key peaks for the allyl and *n*-propyl end groups assigned. The formation of *n*-propyl end groups was not surprising, but the *absence* of any *n*-butyl groups provided key mechanistic evidence that will be discussed shortly. To gain more information regarding initiation, we repeated the previous experiment using triisobutylaluminum/B(C₆F₅)₃ as the cocatalyst. The complicated ^{13}C DEPT spectrum for the polymer is shown in Figure 9c. The peaks assigned in Figure 9a as 4-methyl-butyl signals are present in Figure 9c as well. In addition to this major set of signals, the expected allyl carbons are observed. Also, several smaller signals that may be due to *n*-butyl end groups or impurities in the triisobutylaluminum cocatalyst appear in the spectrum. The peak denoted by the asterisk was not identified but is likely due to a solvent impurity.

Finally, to help verify our assignments, polypropylene made by **1** at 0 °C was hydrogenated using Pd/C, and the ^{13}C DEPT experiment was performed. Figure 9d shows the results of this experiment. All of the signals associated with the allyl end groups disappeared, and four new peaks appeared, corresponding to the formation of *n*-propyl end groups. These new peaks are assigned on the spectrum, and they correspond perfectly to the peaks assigned as *n*-propyl resonances in Figure 9b. Only the peak denoted by the asterisk (compare to Figure 9c) could not be identified.

Scheme 2. Several Processes for the Formation of α-olefin End Groups
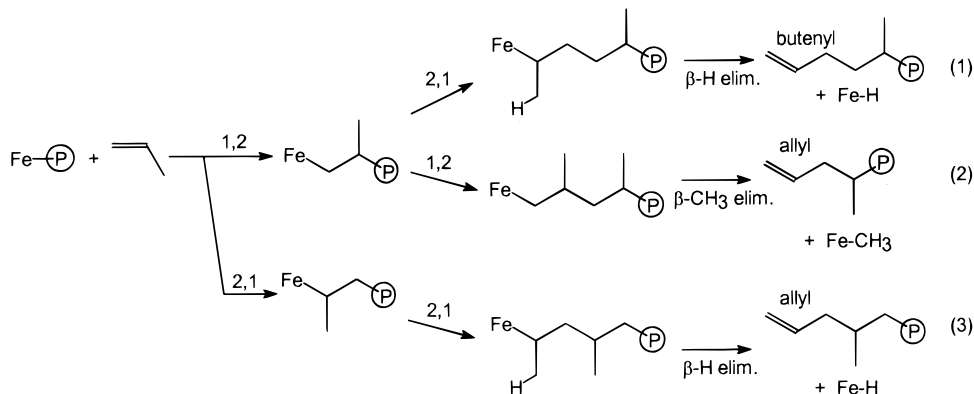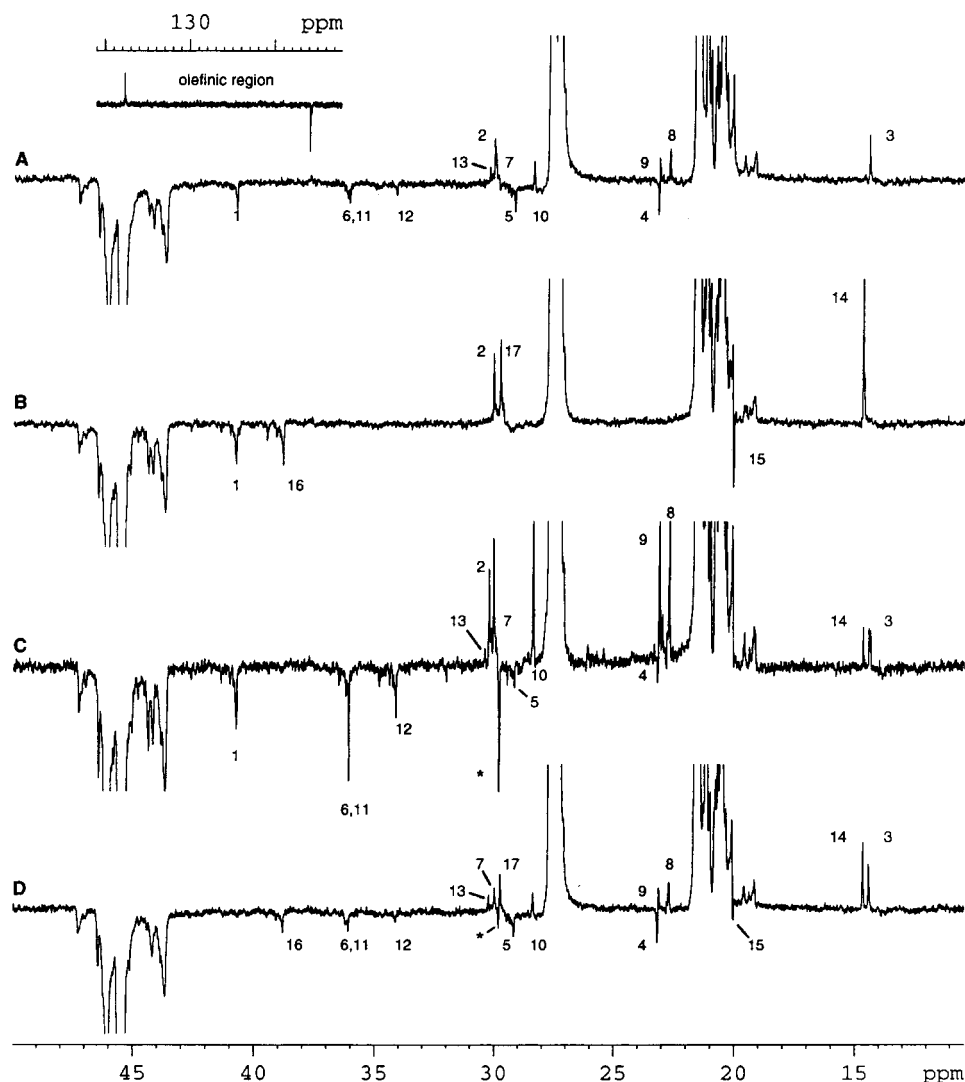
Figure 9. ^{13}C DEPT 135 spectra of end groups generated by propylene polymerization at 0 °C: (a) **1**/MMAO; (b) **1**/AlEt$_3$/(C$_6$F$_5$)$_3$B; (c) **1**/Al(*i*-Bu)$_3$/(C$_6$F$_5$)$_3$B; and (d) **1**/MMAO, followed by hydrogenation of the unsaturated polymer end groups. The peaks are numbered according to the structures shown in Table 4.
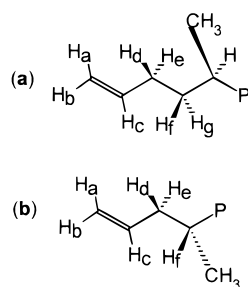
Figure 10. Labeling scheme for hydrogen atoms on (a) a butenyl or (b) an allyl end group.
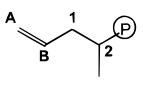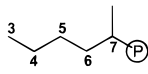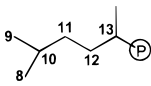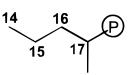
With the observation of allyl end groups at the unsaturated chain ends, *n*-butyl end groups at the saturated chain ends, the variation of the saturated chain ends with activator, and the high regioregularity of the polymerizations, it is possible to propose the mechanism shown in Scheme 3. Neglecting the generation of the active species and the formation of the active catalyst, the catalytic cycle begins with the formation of an Fe−alkyl species made either by β-H abstraction by an incoming monomer from a growing polymer chain or by insertion of propylene into an Fe−H bond following β-H elimination and chain transfer.[35] Either of these

processes occurring in a primary (1,2) fashion would lead to the formation of the Fe−propyl species **10**. The catalyst then undergoes a switch in the regiochemistry, and successive insertions occur in a 2,1 manner, leading to the production of *n*-butyl groups at the saturated chain ends. To the best of our knowledge, these iron catalysts are the first isospecific systems known to operate by a mechanism of 2,1 enchainment.[36] After a number of 2,1 propagation steps leading to species **11**, chain transfer can occur to produce the allyl group at the unsaturated chain end. Regardless of the exact mechanism of chain transfer,[35] the β-H source is always the CH$_3$ group rather than the CH$_2$ group, thus exclusively forming α-olefin in each termination step. The *intensity* of these α-olefin signals also reveals key details about the mechanism. If chain transfer to aluminum were occurring, these signals would be diminished relative to the *n*-butyl signals, because chain transfer to aluminum followed by hydrolysis would lead to an excess of saturated end groups. Thus, chain transfer to aluminum does not appear to be a competitive termination step in propylene polymerization.

To understand why aluminum alkyls do not behave similarly in ethylene[7] and propylene polymerization, it is necessary to consider the interaction of the iron

Table 4. Chemical Shift Values for Polypropylene End Groups

end group	type	carbon	chemical shift ((ppm)
	allyl (C3)	A	115.77
		B	137.65
		1	40.75
		2	30.04
	n-butyl	3	14.42
		4	23.18
		5	29.17
		6	36.10[a]
		7	29.98
	3-methyl-butyl	8	22.70
		9	23.13
		10	28.37
		11	36.10[a]
		12	34.13
		13	30.23
	n-propyl	14	14.66
		15	20.21
		16	38.82
		17	29.76

[a] Carbons 6 and 11 are chemical shift equivalent.

Scheme 3. Mechanism of Initiation, Propagation, and Termination
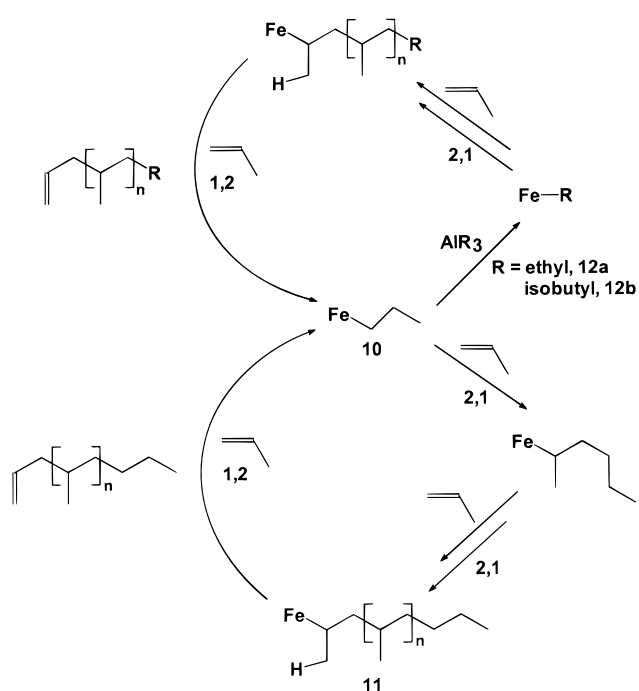
catalysts with different activators. For example, with the tris(perfluorophenyl)borane/AlEt$_3$ cocatalyst, *n*-propyl end groups were observed. We interpret these results by employing the top portion of Scheme 3, in which the Fe−propyl complex **10** undergoes chain transfer to the triethylaluminum to generate the Fe−ethyl complex **12a**. The 2,1 insertion of this Fe−ethyl complex leads to the production of *n*-propyl end groups at the saturated chain ends and, following chain transfer, allyl groups at the unsaturated ends. Thus, it also seems likely from this result that propylene prefers to

insert into Fe−H bonds in a primary fashion (1,2) but that Fe−alkyls cause the monomer to insert with 2,1 regiochemistry. Both MMAO and triisobutylaluminum are able to transfer isobutyl groups to **10** to form **12b**, which propagates via the same mechanism to give 3-methyl-butyl end groups. Apparently, triethylaluminum is more effective than MMAO or triisobutylaluminum at exchanging with the Fe−propyl species, as evidenced by the single set of end groups identifiable in Figure 9b. Also, it appears that the methyl groups from MMAO are not involved in these exchange processes, because no signals in Figure 9a could be identified as ethyl (*sec*-butyl) end groups. From this work, it is reasonable to propose that the aluminum alkyl cocatalysts *do not* undergo exchange with *secondary* Fe−alkyls, but they can readily exchange with *primary* Fe−alkyls. This difference in reactivity allows the saturated end groups of the polymer to be modified based on the aluminum cocatalyst chosen, but only propenyl end groups, resulting from β-H elimination following 2,1 insertion, are observed at the unsaturated chain ends. The proposal that aluminum alkyls exchange only with primary Fe−alkyls is in agreement with the observation that this reaction is a significant chain transfer process in polymerization of ethylene by these catalysts.[6,7b]

Conclusions

The iron complexes reported herein represent a new class of isospecific propylene polymerization catalysts. These catalysts are unique in several ways. First, they are the first late-metal systems known to polymerize propylene in an isotactic fashion.[9] Regardless of catalyst structure, the isotacticity is governed by a chain-end control mechanism. Second, chain propagation proceeds through 2,1 insertion of monomer, making these the first isospecific propylene polymerization catalysts that operate via a secondary enchainment mechanism. Third, the polymer end groups resulting from termination consist solely of 1-propenyl groups, making these the first systems to produce only α-olefin end groups by β-H elimination from the growing polypropylene chains.[36,37] Fourth, these polymers are highly regioregular, with regioerrors occurring only in the lower molecular weight polymers made by the complexes with reduced steric bulk. Finally, the polymer end groups observed at the saturated chain ends are dependent on the activator used, presumably because of a mechanism in which the primary Fe−propyl complexes formed after chain transfer can undergo alkyl exchange with the Al−alkyl cocatalysts. Apparently, these alkyl exchange processes are only possible with primary Fe−alkyl species because no decrease in the olefinic signals is observed, as would be expected by chain transfer of secondary Fe−alkyls to aluminum followed by hydrolysis to form saturated end groups. We are currently investigating further modifications of catalyst structure and activators and the effects of changes in reaction conditions on the tacticities, TOFs, TONs, and molecular weights of the polymers.

Experimental Section

General Considerations. All manipulations of air-, water-, or air/water-sensitive compounds were performed using standard high-vacuum or Schlenk techniques. Argon and nitrogen were purified by passage through columns of BASF R3-11 catalyst (Chemalog) and 4-A molecular sieves. Elemental

analyses were performed by Atlantic Microlab, Inc., of Norcross, GA. GPC data were obtained using polystyrene standards and universal calibration methods.

Materials. Toluene was degassed and passed over activated alumina (Brockman I) prior to use. THF was distilled from sodium/benzophenone. Anhydrous methanol was purchased from Mallinckrodt and used without further purification; 2-propanol was not dried prior to use. A 7% weight solution of modified MAO (MMAO) in heptane was purchased from Akzo Nobel. Triethylaluminum and triisobutylaluminum solutions in toluene, 97% formic acid, iron(II) chloride tetrahydrate, 2,6-diacetylpyridine, and all alkyl-substituted anilines were purchased from Aldrich and used without further purification. Polymer grade propylene was purchased from National Specialty Gases and used without further purification.

Synthesis of Ligands 4′ − 9′ 2-[1-(2-*tert*-Butylphenyl-imino)ethyl]-6-[1-(2,6-dimethylphenylimino)ethyl]pyri-dine (4′). 2,6-Diacetylpyridine (1.0 g, 6.1 mmol) and 2-*tert*-butylaniline (0.96 mL, 6.7 mmol) were dissolved in 20 mL of methanol in a round-bottom flask. One drop of 97% formic acid was added, and the solution was stirred in the sealed flask for 2 days at 25 °C. A yellow solid (1.57 g, 87%) was collected, washed with cold methanol, and identified as the desired monoimine by ^{1}H NMR. This monoimine (500 mg) was dissolved in 25 mL of hot isopropyl alcohol, followed by the addition of five drops of 97% formic acid and excess 2,6-dimethylaniline. The solution was stirred in the sealed flask at 70 °C for 4 days, followed by removal of the alcohol in vacuo. The remaining oil was redissolved in hot methanol and slowly cooled to 25 °C , during which time 145 mg of a yellow solid formed. This solid was determined to be 90% desired product **4′** and 10% ligand **2′** by ^{1}H NMR. ^{1}H NMR (CDCl$_3$) δ 8.64 (d, 1, Py−H_m), 8.44 (d, 1, Py−H_m), 7.95 (t, 1, Py−H_p), 7.42 (d, 1, H_{aryl}), 7.17 (t, 1, H_{aryl}), 7.04 (m, 4, H_{aryl}), 6.53 (d, 1, H_{aryl}), 2.39 (s, 3, N=CMe), 2.39 (s, 3, N=CMe), 2.08 (s, 6, ArMe), 1.34 (s, 9, *t-Bu*).

2-[1-(2-*tert*-Butylphenylimino)ethyl]-6-[1-(2,6-diisopro-pylphenylimino)ethyl]pyridine (5′). 2,6-Diacetylpyridine (1.0 g, 6.1 mmol) and 2,6-diisopropylaniline (1.2 mL, 6.4 mmol) were dissolved in 100 mL of methanol in a round-bottom flask. Five drops of 97% formic acid were added, and the solution was stirred in the sealed flask for 2 days at 25 °C. Yellow solid (707 mg; 35.8%) was collected by filtration and dissolved in hot isopropyl alcohol to remove the diimine **1′** byproduct. The solution was refiltered, and the alcohol was removed to give 622 mg (31.5%) of the desired monoimine. Monoimine (300 mg, 0.9 mmol) and excess 2-*tert*-butylaniline were dissolved in 20 mL of hot isopropyl alcohol in a round-bottom flask. Five drops of 97% formic acid were added, and the solution was stirred in the sealed flask at 75 °C for 18 h. The solution was allowed to cool, and 145 mg of impure product was isolated by filtration. The filtrate was cooled to −30 °C, and 233 (55%) mg of crystals suitable for X-ray analysis were collected and identified as the desired **5′**. ^{1}H NMR (CDCl$_3$) δ 8.42 (d, 1, Py−H_m), 8.39 (d, 1, Py−H_m), 7.90 (t, 1, Py−H_p), 7.40 (d, 1, H_{aryl}), 7.12 (m, 5, H_{aryl}), 6.53 (d, 1, H_{aryl}), 2.78 (septet, 2, CHMe$_2$), 2.38 (s, 3, N=CMe), 2.24 (s, 3, N=CMe), 1.35 (s, 9, *t-Bu*), 1.13 (d, 12, CHMe_2); ^{13}C NMR (CDCl$_3$, upfield region) δ 35.2, 29.7, 28.2, 23.2, 22.8, 16.8. Anal. Calcd for C$_{31}$H$_{39}$N$_3$: C, 82.07; H, 8.66; N, 9.26. Found: C, 81.79; H, 8.55; N, 9.38.

2,6-bis[1-(2-Isopropyl-6-methylphenylimino)ethyl]-pyridine (6′). 2,6-Diacetylpyridine (600 mg, 3.7 mmol) and 2-isopropyl-6-methylaniline (2.0 mL, 12.8 mmol) were dissolved in 50 mL of methanol in a round-bottom flask. Five drops of 97% formic acid were added, and the solution was allowed to stir in the sealed flask at 55 °C for 24 h. An off-white solid (800 mg; 51.2%) was collected by filtration and identified as the desired **6′**. An additional crop of solid was collected and identified as 80% pure monoimine byproduct. ^{1}H NMR of **6′** (CDCl$_3$) δ 8.46 (d, 2, Py−H_m), 7.90 (t, 1, Py−H_p), 7.16 (d, 2, H_{aryl}), 7.04 (m, 4, H_{aryl}), 2.82 (septet, 2, CHMe$_2$), 2.24 (s, 6, N=CMe), 2.02 (s, 6, ArMe), 1.18 (d, 6, CHMe), 1.13 (d, 6, CHMe); ^{13}C NMR (CDCl$_3$, upfield region) δ 28.4, 23.1, 22.9, 18.2, 16.8. Anal. Calcd for C$_{29}$H$_{35}$N$_3$: C, 81.84; H, 8.29; N, 9.87. Found: C, 81.54; H, 8.24; N, 9.76.

2-[1-(2,6-Diisopropylphenylimino)ethyl]-6-[1-(2,6-di-methylphenylimino)ethyl]pyridine (7′). Monoimine (300 mg) formed in the preparation of **5′** was dissolved with excess 2,6-dimethylaniline in hot isopropyl alcohol in a round-bottom flask. Five drops of 97% formic acid were added, and the solution was allowed to stir in the sealed flask at 75 °C for 4 days. The solvent was removed, and the residue was frozen at −30 °C and then washed with cold methanol to give 65 mg (16.8%) of the desired **7′**. ^{1}H NMR (CDCl$_3$) δ 8.45 (d, 1, Py−H_m), 8.44 (d, 1, Py−H_m), 7.89 (t, 1, Py−H_p), 7.10 (m, 5, H_{aryl}), 6.92 (dd, 1, H_{aryl}), 2.74 (septet, 2, CHMe$_2$), 2.24 (s, 3, N=CMe), 2.22 (s, 3, N=CMe), 2.03 (s, 6, ArMe), 1.13 (d, 12, CHMe_2); ^{13}C NMR (CDCl$_3$, upfield region) δ 28.3, 23.2, 22.9, 18.0, 17.2, 16.5; MS FAB$^+$ m/z = 426.

2,6-bis(2-Isopropyl-6-methylphenylimino)methylpyri-dine (8′). 2,6-Pyridinedicarboxaldehyde (210 mg, 1.6 mmol) and 2-isopropyl-6-methylaniline (0.6 mL, 3.8 mmol) were dissolved in 20 mL of methanol in a round-bottom flask. Three drops of 97% formic acid were added, and the solution was allowed to stir in the sealed flask for 2 h. An off-white solid (471 mg; 76.2%) was collected by filtration and identified as the desired **8′**. ^{1}H NMR (CDCl$_3$) δ 8.38 (d, 2, Py−H_m), 8.36 (s, 2, N=CH), 7.98 (t, 1, Py−H_p), 7.17 (dd, 2, H_{aryl}), 7.06 (m, 4, H_{aryl}), 3.03 (septet, 2, CHMe$_2$), 2.15 (s, 6, ArMe), 1.18 (d, 6, CHMe); ^{13}C NMR (CDCl$_3$, upfield region) δ 28.0, 23.2, 18.7. Anal. Calcd for C$_{27}$H$_{31}$N$_3$: C, 81.67; H, 7.86; N, 10.57. Found: C, 81.56; H, 7.83; N, 10.54.

2-[1-(2,6-Diisopropylphenylimino)ethyl]-6-[1-(2-isopro-pyl-6-methylphenylimino)ethyl]pyridine (9′). The 80% pure monoimine byproduct (700 mg) formed in the preparation of **6′** was dissolved with excess 2,6-diisopropylaniline (2.0 mL) in 50 mL of methanol in a round-bottom flask. Five drops of 97% formic acid were added, and the solution was stirred for 2 days in the sealed flask. A yellow solid (988 mg; 95% pure, with 5% **6′** impurity) was collected and identified as the desired **9′**. ^{1}H NMR (CDCl$_3$) δ 8.56 (d, 2, Py−H_m), 7.98 (t, 1, Py−H_p), 7.20 (m, 6, H_{aryl}), 2.85 (m, 3, CHMe$_2$), 2.34 (s, 3, N=CMe), 2.33 (s, 3, N=CMe), 2.12 (s, 3, ArMe), 1.23 (m, 18, CHMe_2); ^{13}C NMR (CDCl$_3$, upfield region) δ 28.3, 23.3, 23.2, 22.9, 18.2, 17.2, 17.1, 16.9, 16.8 (Note: There are actually 12 different carbons for this ligand, but this number is reduced to 9 if the 2 aryl rings are assumed to have no chemical shift effect on each other; this is a reasonable assumption considering the similar substitution patterns on the rings. Anal. Calcd for C$_{31}$H$_{39}$N$_3$: C, 82.07; H, 8.66; N, 9.26. Found: C, 81.28; H, 8.59; N, 9.05.

Synthesis of Complexes 4−9. Under an inert atmosphere, 1.05 equiv of the appropriate ligand and 1.0 equiv of FeCl$_2$·4H$_2$O were stirred with dry THF for 2 h, resulting in the formation of a deep blue solution or suspension. If the target complex was soluble in THF, the solvent was removed in vacuo, and the remaining solid was washed in air with ether and pentane. If a suspension formed, then pentane was added to the reaction flask, and the solids were filtered in air and washed with ether and pentane. All of the complexes were isolated in near quantitative yields. All of the reported complexes were either deep blue or purple, except for **8** which was gray-purple.

Polymerization Procedure. The precatalyst complex, including the borane cocatalyst if applicable, was weighed out and added to a flame-dried Schlenk flask with a stirbar. The flask was back-filled three times with propylene, then charged with 50 mL of toluene. Stirring was begun, and after the formation of an evenly dispersed suspension and equilibration of the solvent temperature, the aluminum cocatalyst was added via syringe. The polymerization was quenched with acidified methanol, and the polymer was isolated either by filtration or by evaporation of the solvent and dissolution of the remaining polymer in hot hexane followed by filtration to remove any remaining aluminum salts. Refer to Table 1 for information regarding catalyst loadings, reaction lengths, and polymerization temperatures.

Hydrogenation of Polypropylene. Polypropylene (500 mg) made by complex **1**/MMAO (Table 1, entry 2) was weighed out and added to a 100 mL round-bottom flask that contained

10 mg of a 10% Pd/C powder. Diethyl ether (20 mL) was added to the flask to dissolve the polymer, and the flask was fitted with a septum and purged with H₂ for 5 min with stirring. The purge was discontinued, and the flask was charged with 60 mL of H₂ to create a pressure slightly higher than 1 atm. Stirring was continued for 24 h, followed by filtration and removal of the solvent. ¹H NMR spectroscopy showed no olefinic resonances.

NMR Experiments. ¹³C NMR data were obtained by two methods. For examination of the methyl pentad region, a Bruker AMX 500 MHz instrument was used. Polypropylene (100 mg) was dissolved in 1.7 mL of d_5-bromobenzene in a 10 mm o.d. tube. At 100 °C, 1000 transients were collected, using a 2.16 s acquisition time and a 66° pulse angle. To examine the end groups via ¹³C DEPT 135 experiments, a Bruker Avance 400 MHz instrument was used. Polypropylene (100 mg) was dissolved in 0.7 mL of 1,2-dideuterio-1,1,2,2-tetrachloroethane in a 5 mm o.d. tube. At 25 °C, 1000 transients were collected, using a 1.032 s acquisition time and a 4.0 s relaxation delay. The proton decoupling experiments were performed on a Bruker Avance 400 MHz instrument. All spectra were referenced to TMS.

Supporting Information Available: Crystallographic data and collection parameters and atomic coordinates for **5′** and **6a** (7 pages). Ordering and accessing information is given on any current masthead page.

References and Notes

(1) For recent reviews, see: (a) Brintzinger, H. H.; Fischer, D.; Mülhaupt, R.; Rieger, B.; Waymouth, R. *Angew. Chem., Int. Ed. Engl.* **1995**, *34*, 1143. (b) Bochmann, M. *J. Chem. Soc., Dalton Trans.* **1996**, 255. (c) Kaminsky, W.; Arndt, M. *Adv. Polym. Sci.* **1997**, *127*, 143. (d) Möhring, P. C.; Coville, N. J. *J. Organomet. Chem.* **1994**, *479*, 1. (e) Fink, G., Mülhaupt, R., Brintzinger, H. H., Eds. *Ziegler Catalysts: Recent Scientific Innovations and Technological Improvement*; Springer–Verlag: Berlin, 1995.

(2) (a) Busico, V.; Cipullo, R.; Chadwick, J. C.; Modder, J. F.; Sudmeijer, O. *Macromolecules* **1994**, *27*, 7538. (b) Asakura, T.; Nakayama, N.; Demura, M.; Asano, A. *Macromolecules* **1992**, *25*, 4876. (c) Zambelli, A.; Tosi, C. *Adv. Polym. Sci.* **1974**, *15*, 31. (d) Grassi, A.; Zambelli, A.; Resconi, L.; Albizzati, E.; Mazzocchi, R. *Macromolecules* **1988**, *21*, 617. (e) Guerra, G.; Longo, P.; Corradini, P.; Resconi, L. *J. Am. Chem. Soc.* **1997**, *119*, 4394. (f) Ewart, S. W.; Sarsfield, M. J.; Jeremic, D.; Tremblay, T. L.; Williams, E. F.; Baird, M. C. *Organometallics* **1998**, *17*, 1502.

(3) (a) Spalek, W.; Küber, F.; Winter, A.; Rohrmann, J.; Bachmann, B.; Antberg, M.; Dolle, V.; Paulus, E. *Organometallics* **1994**, *13*, 954. (b) Spalek, W.; Antberg, M.; Rohrmann, J.; Winter, A.; Bachmann, B.; Kiprof, P.; Behm, J.; Hermann, W. *Angew. Chem., Int. Ed. Engl.* **1992**, *31*, 1347. (c) Resconi, L.; Jones, R. L.; Rheingold, A. L.; Yap, G. P. A. *Organometallics* **1996**, *15*, 998.

(4) (a) Coates, G. W.; Waymouth, R. M. *Science* **1995**, *267*, 217. (b) Bruce, M. D.; Coates, G. W.; Hauptman, E.; Waymouth, R. M.; Ziller, J. W. *J. Am. Chem. Soc.* **1997**, *119*, 11174. (c) Hauptman, E.; Waymouth, R. M.; Ziller, J. W. *J. Am. Chem. Soc.* **1995**, *117*, 11586. (d) Mallin, D. T.; Rausch, M. D.; Lin, Y. G.; Dong, S.; Chien, J. C. W. *J. Am. Chem. Soc.* **1990**, *112*, 2030. (e) Llinas, G. H.; Rausch, M. D.; Lin, G.-Y.; Winter, H. H.; Atwood, J. L.; Bott, S. G.; Chien, J. C. W. *J. Am. Chem. Soc.* **1991**, *113*, 8569. (f) Golab, J. T. *Chemtech* **1998**, *28*, 17.

(5) (a) Killian, C. M.; Tempel, D. T.; Johnson, L. K.; Brookhart, M. *J. Am. Chem. Soc.* **1996**, *118*, 11664. (b) McClain, S. J.; McCord, E. F.; Johnson, L. K.; Ittel, S. D.; Nelson, L. T. J.; Arthur, S. D.; Halfhill, M. J.; Teasley, M. F.; Tempel, D. J.; Killian, C. M.; Brookhart, M. *Polym. Prepr. (Am. Chem. Soc., Div. Polym. Chem.)* **1997**, *38*, 772. (c) Nelson, L. T. J.; McCord, E. F.; Johnson, L. K.; McClain, S. J.; Ittel, S. D.; Killian, C. M.; Brookhart, M. *Polym. Prepr. (Am. Chem. Soc., Div. Polym.*

Chem.) **1997**, *38*, 133. (d) Johnson, L. K.; Killian, C. M.; Arthur, S. D.; Feldman, J.; McCord, E. F.; McClain, S. J.; Kreutzer, K. A.; Bennett, A. M. A.; Coughlin, E. B.; Ittel, S. D.; Parthasarathy, A.; Tempel, D. J.; Brookhart, M. (DuPont/UNC) World Patent Application 96/23010, 1996.

(6) Britovsek, G. J. P.; Gibson, V. C.; Kimberley, B. S.; Maddox, P. J.; McTavish, S. J.; Solan, G. A.; White, A. J. P.; Williams, D. J. *Chem. Commun.* **1998**, 849.

(7) (a) Bennett, A. M. A. (DuPont) World Patent Application 98/27124, 1998. (b) Small, B. L.; Brookhart, M.; Bennett, A. M. A. *J. Am. Chem. Soc.* **1998**, *120*, 4049.

(8) Small, B. L.; Brookhart, M. *J. Am. Chem. Soc.* **1998**, *120*, 7143.

(9) (a) Small, B. L.; Brookhart, M. *Polym. Prepr. (Am. Chem. Soc., Div. Polym. Chem.)* **1998**, *39*, 213. (b) Brookhart, M.; Small, B. L. (UNC) World Patent Application 98/30612, 1998.

(10) MMAO is the same as MAO except for the substitution of 25% of the methyl groups with isobutyl groups. MMAO has the advantage of increased shelf life, but as is discussed in this paper, these isobutyl groups can affect the composition of the polymer end groups.

(11) (a) Johnson, L. K.; Killian, C. M.; Brookhart, M. *J. Am. Chem. Soc.* **1995**, *117*, 6414. (b) Killian, C. M.; Johnson, L. K.; Brookhart, M. *Organometallics* **1997**, *16*, 2005.

(12) (a) Peebles, L. H., Jr. *Molecular Weight Distributions in Polymers;* Wiley-Interscience: New York, 1971. (b) Flory, P. J. *Principles of Polymer Chemistry*; Cornell University Press: Ithaca, N. Y., 1953.

(13) Marks, T. J. *Acc. Chem. Res.* **1992**, *25*, 57. (b) Resconi, L.; Piemontesi, F.; Fransiscono, G.; Abis, L.; Fiorani, T. *J. Am. Chem. Soc.* **1992**, *114*, 1025. (c) Giardello, M. A.; Eisen, M. S.; Stern, C. L.; Marks, T. J. *J. Am. Chem. Soc.* **1995**, *117*, 12144. (d) Marques, M. V.; Nunes, P. C.; Tait, P. J. T.; Dias, A. R. *J. Polym. Sci.; Part A* **1993**, *31*, 219. (e) Komiya, S.; Katoh, M.; Ikariya, T.; Grubbs, R. H.; Yamamoto, T.; Yamamoto, A. *J. Organomet. Chem.* **1984**, *260*, 115.

(14) Ewen, J. A. *J. Am. Chem. Soc.* **1984**, *106*, 6355.

(15) Bovey, F. A. *J. Polym. Sci.* **1960**, *44*, 173.

(16) (a) Doi, Y.; Asakuru, T. *Makromol. Chem.* **1975**, *176*, 507. (b) Sheldon, R. A.; Fueno, T.; Tsunstsugu; Kurukawa, J. *J. Polym. Sci., Part B* **1965**, *3*, 23. (c) Xu, J.; Feng, L.; Yang, S. *Macromolecules* **1997**, *30*, 2539.

(17) There are numerous examples in the literature of complexes whose stereospecific behavior changes with modifications in the reaction conditions. See refs 1 and 14.

(18) (a) Wild, F. R. W. P.; Zsolani, L.; Huttner, G.; Brintzinger, H. H. *J. Organomet. Chem.* **1982**, *232*, 233. (b) Wild, F. R. W. P.; Wasiucionek, M.; Huttner, G.; Brintzinger, H. H. *J. Organomet. Chem.* **1985**, *288*, 63. (c) Kaminsky, W.; Külper, K.; Brintzinger, H. H.; Wild, F. R. W. P. *Angew. Chem., Int. Ed. Engl.* **1985**, *24*, 507.

(19) (a) Ewen, J. A.; Elder, M. J.; Jones, R. L.; Haspeslagh, L.; Atwood, J. L.; Bott, S. G.; Robinson, K. *Makromol. Chem., Macromol. Symp.* **1991**, *48/49*, 253. (b) Ewen, J. A.; Haspeslagh, L.; Atwood, J. L.; Zang, H. *J. Am. Chem. Soc.* **1987**, *109*, 6544. (c) Ewen, J. A.; Jones, R. L.; Razavi, A.; Ferrara, J. D. *J. Am. Chem. Soc.* **1988**, *110*, 6255.

(20) Sinn, H.; Kaminsky, W. *Adv. Organomet. Chem.* **1980**, *18*, 99. (b) Kaminsky, W.; Miri, M.; Sinn, H.; Woldt, R. *Makromol. Chem., Rapid Commun.* **1983**, *4*, 417. (c) Soga, K.; Shiono, T.; Takemura, S.; Kaminsky. W. *Makromol. Chem., Rapid Commun.* **1987**, *8*, 305.

(21) (a) Herzog, T. A.; Zubris, D. L.; Bercaw, J. E. *J. Am. Chem. Soc.* **1996**, *118*, 11988. (b) Coughlin, E. B.; Bercaw, J. E. *J. Am. Chem. Soc.* **1992**, *114*, 7606. (c) Bierwagen, E. P.; Bercaw, J. E.; Goddard, W. A. *J. Am. Chem. Soc.* **1994**, *116*, 1481. (d) Mitchell, J. P.; Hajela, S.; Brookhart, S. K.; Hardcastle, K. I.; Henling, L. M.; Bercaw, J. E. *J. Am. Chem. Soc.* **1996**, *118*, 1045.

(22) (a) Averbuj, C.; Tish, E.; Eisen, M. S. *J. Am. Chem. Soc.* **1998**, *120*, 8640. (b) Volkis, V.; Shmulinson, M.; Averbuj, C.; Lisovskii, A.; Edelmann, F. T.; Eisen, M. S. *Organometallics* **1998**, *3155*, 5. (c) Chen, Y.-X.; Metz, M. V.; Li, L.; Stern, C. L.; Marks, T. J. *J. Am. Chem. Soc.* **1998**, *6287*, 7. (d) Gauthier, W. J.; Collins, S. *Macromolecules* **1995**, *28*, 3779. (e) van der Leek, Y.; Angermund, K.; Reffke, M.; Kleinschmidt, R.; Goretzki, R.; Fink, G. *Chem. Eur. J.* **1997**, *3*, 585.

(23) Crystal data of **5′**: monoclinic, *P*2₁/*c*, yellow; a = 8.7202(8) Å, b = 20.5203(18) Å, c = 15.9434(10) Å; V = 2758.4(4) Å³; Z = 4; R = 0.044; GOF = 1.62.

(24) (a) Tempel, D. J. Doctoral Dissertation, University of North Carolina at Chapel Hill, 1998. (b) Svejda, S. A.; Brookhart, M. Unpublished results.

(25) Crystal data of **6a**: monoclinic, *P*21/*c*, blue; *a* = 12.0671(9) Å, *b* = 16.5136(13) Å, *c* = 16.5081(12) Å; *V* = 3254.9(4) Å³; *Z* = 4; *R* = 0.088; GOF = 4.90. Crystals of **6a** were grown by allowing pentane to slowly diffuse into a solution of the complex in chlorobenzene.

(26) We have found that exposure of the iron complexes to halogenated solvents results in greatly exaggerated magnetic susceptibility values and greatly reduced activities. These observations are consistent with free-radical reactions leading to the formation of Fe(III) species and catalytically inactive impurities.

(27) Complex **3**, for which atom connectivity data were obtained from crystals grown in CH_2Cl_2/pentane, contains a second iron center with a bridging Cl atom. In the case of **6a**, monovalent OH^- is more analogous than oxide to Cl^-.

(28) For leading references relating to a variety of migratory insertion processes and polymerization systems, see: (a) Tempel, D. J.; Brookhart, M. *Organometallics* **1998**, *17*, 2290. (b) Lee, H.; Hascall, T.; Desrosiers, P. J.; Parkin, G. *J. Am. Chem. Soc.* **1998**, *120*, 5830. (c) Brookhart, M.; Hauptman, E.; Lincoln, D. M. *J. Am. Chem. Soc.* **1992**, *114*, 10394. (d) Brookhart, M.; Lincoln, D. M.; Volpe, A. F.; Schmidt, G. F. *Organometallics* **1989**, *8*, 1212. (e) Green, M. L. H.; Sella, A.; Wong, L.-L. *Organometallics* **1992**, *11*, 2650. (f) Mecking, S.; Johnson, L. K.; Wang, L.; Brookhart, M. *J. Am. Chem. Soc.* **1998**, *120*, 888. (g) Rix, F. C.; Brookhart, M.; White, P. S. *J. Am. Chem. Soc.* **1996**, *118*, 2436.

(29) (a) Cheng, H. N.; Smith, D. A. *Macromolecules* **1986**, *19*, 2065. (b) Carvill, A.; Zetta, L.; Zannoni, G.; Sacchi, M. C. *Macromolecules* **1998**, *31*, 3783.

(30) (a) Eshuis, J.; Tan, Y.; Teuben, J. H.; Renkema, J. *J. Mol. Catal.* **1990**, *62*, 277. (b) Eshuis, J.; Tan, Y.; Meetsma, A.; Teuben, J. H. *Organometallics* **1992**, *11*, 362. (c) Yang, X.; Stern, C. L.; Marks, T. J. *Angew. Chem., Int. Ed. Engl.* **1992**, *31*, 1375. (d) Mise, T.; Kageyama, A.; Miya, S.; Yamazaki, H. *Chem. Lett.* **1991**, 1525. (e) Kesti, M.; Waymouth, R. M. *J. Am. Chem. Soc.* **1992**, *114*, 3565. (f) Guo, Z.; Swenson, D.; Jordan, R. *Organometallics* **1994**, *13*, 1424. (g) Hajela, S.; Bercaw, J. E. *Organometallics* **1994**, *13*, 1147. (h) Yang, X.;

Stern, C. L.; Marks, T. J. *J. Am. Chem. Soc.* **1994**, *116*, 10015.

(31) (a) C3 of 1-hexene, which would be a reasonable model for a *butenyl* end group, has a ¹³C NMR chemical shift of 33.5 ppm. (b) For a discussion of ¹³C NMR alkyl substituent effects in branched hydrocarbons, see: Silverstein, R. M.; Bassler, G. C.; Morrill, T. C. *Spectrometric Identification of Organic Compounds*, 5th ed.; John Wiley & Sons: New York, 1991; Chapter 5.

(32) Zambelli, A.; Locatelli, P.; Bajo, G.; Bovey, F. A. *Macromolecules* **1975**, *8*, 687.

(33) Zambelli, A.; Locatelli, P.; Bajo, G. *Macromolecules* **1979**, *12*, 154.

(34) Hayashi, T.; Inoue, Y.; Chûjô, R.; Asakura, T. *Macromolecules* **1988**, *21*, 2675.

(35) β-H transfer to the incoming monomer to generate a new Fe—alkyl species, or to the metal to form an Fe—H species, are both possible routes for chain transfer. If β-H transfer to monomer occurs, it must occur in a primary (1,2) fashion (opposite the regiochemistry observed for propagation) to generate an Fe—propyl complex.

(36) Soluble vanadium catalysts based on VCl_4/Et_2AlCl will polymerize propylene at −78 °C in a 2,1 fashion to generate *syndiotactic* polypropylene. These systems are not highly regioregular, and the polymer chains apparently do not terminate via β-H elimination to give unsaturated end groups suitable for NMR analysis. For example, see: (a) Doi, Y. *Macromolecules* **1979**, *12*, 248. (b) Zambelli, A.; Allegra, G. *Macromolecules* **1980**, *13*, 42. (c) Ammendola, P.; Shijing, X.; Grassi, A.; Zambelli, A. *Gazz. Chim. Ital.* **1988**, *118*, 769. (d) Zambelli, A.; Léty, A.; Tosi, C.; Pasquon, I. *Makromol. Chem.* **1968**, *115*, 73. (e) Zambelli, A.; Giongo, M. G.; Natta, G. *Makromol. Chem.* **1968**, *112*, 183.

(37) Note added in proof. Analysis of polypropylene made from catalyst **1**/methylalumoxane has recently been reported: Pellecchia, C.; Mazzeo, M.; Pappalardo, D. *Macromol. Rapid Commun.* **1998**, *19*, 651.